LINC-NIRVANA for the LBT: Setting up the world's largest NIR binoculars for astronomy

Ralph Hofferbert*[a], Harald Baumeister[a], Thomas Bertram[a], Jürgen Berwein[a], Peter Bizenberger[a], Armin Böhm[a], Michael Böhm[a], José Luis Borelli[a], Matthieu Brangier[a], Florian Briegel[a], Albert Conrad[a], Fulvio De Bonis[a], Roman Follert[a], Tom Herbst[a], Armin Huber[a], Frank Kittmann[a], Martin Kürster[a], Werner Laun[a], Ulrich Mall[a], Daniel Meschke[a], Lars Mohr[a], Vianak Naranjo[a], Aleksei Pavlov[a], Jörg-Uwe Pott[a], Hans-Walter Rix[a], Ralf-Rainer Rohloff[a], Eva Schinnerer[a], Clemens Storz[a], Jan Trowitzsch[a], Zhaojun Yan[a], Xianyu Zhang[a]; Andreas Eckart[b], Matthew Horrobin[b], Steffen Rost[b], Christian Straubmeier[b], Imke Wank[b], Jens Zuther[b]; Udo Beckmann[c], Claus Connot[c], Matthias Heininger[c], Karl-Heinz Hofmann[c], Tim Kröner[c], Eddy Nussbaum[c], Dieter Schertl[c], Gerd Weigelt[c]; Maria Bergomi[d], Alessandro Brunelli[d], Marco Dima[d], Jacopo Farinato[d], Demetrio Magrin[d], Luca Marafatto[d], Roberto Ragazzoni[d], Valentina Viotto[d]; Carmelo Arcidiacono[e], Giovanni Bregoli[e], Paolo Ciliegi[e], Guiseppe Cosentino[e], Emiliano Diolaiti[e], Italo Foppiani[e], Matteo Lombini[e], Laura Schreiber[e]; Francesco D'Alessio[f], Gianluca Li Causi[f], Dario Lorenzetti[f], Fabrizio Vitali[f]; Mario Bertero[g], Patrizia Boccacci[g], Andrea La Camera[g].

[a]Max-Planck-Institut für Astronomie (MPIA), Königstuhl 17, D-69117 Heidelberg, Germany;
[b]I. Physikalisches Institut, Universität zu Köln, Zülpicher Strasse 77, D-50937 Köln, Germany;
[c]Max-Planck-Institut für Radioastronomie (MPIfR), Auf dem Hügel 69, D-53121 Bonn, Germany;
[d]INAF - Osservatorio Astronomico di Padova, Vicolo dell'Osservatorio 5, I-35122 Padova, Italy;
[e]INAF - Osservatorio Astronomico di Bologna, Via Ranzani 1, I-40127 Bologna, Italy;
[f]INAF - Osservatorio Astronomico di Roma, Via di Frascati 33, I-00040 Monteporzio Catone, Italy;
[g]DISI, Università degli Studi di Genova, Via Dodecaneso 35, I-16146 Genova, Italy.

ABSTRACT

LINC-NIRVANA (LN) is the near-infrared, Fizeau-type imaging interferometer for the Large Binocular Telescope (LBT) on Mt. Graham, Arizona, USA (3267m of elevation). The instrument is currently being built by a consortium of German and Italian institutes under the leadership of the Max Planck Institute for Astronomy (MPIA) in Heidelberg, Germany. It will combine the radiation from both 8.4m primary mirrors of LBT in such a way that the sensitivity of a 11.9m telescope and the spatial resolution of a 22.8m telescope will be obtained within a 10.5arcsec x 10.5arcsec scientific field of view. Interferometric fringes of the combined beams are tracked in an oval field with diameters of 1 and 1.5arcmin. In addition, both incoming beams are individually corrected by LN's multi-conjugate adaptive optics (MCAO) system to reduce atmospheric image distortion over a circular field of up to 6arcmin in diameter.

This paper gives a comprehensive technical overview of the instrument comprising the detailed design of LN's four major systems for interferometric imaging and fringe tracking, both in the NIR range of 1 - 2.4µm, as well as atmospheric turbulence correction at two altitudes, both in the visible range of 0.6 - 0.9µm. The resulting performance capabilities and a short outlook of some of the major science goals will be presented. In addition, the roadmap for the related assembly, integration and verification (AIV) process will be discussed. To avoid late interface-related risks, strategies for early hardware as well as software interactions with the telescope have been elaborated. The goal is to ship LN to the LBT in 2014.

Keywords**:** LINC-NIRVANA, Large Binocular Telescope, LBT, Fizeau interferometry, sparse aperture imaging, multi-conjugate adaptive optics, MCAO, fringe tracking, deformable mirror

*hofferbert@mpia.de; phone 49 6221 528-209; fax 49 6221 528-246; mpia.de

1. INTRODUCTION

In 1988, it was decided to build a new large telescope facility in the northern hemisphere with the goal to reach sensitivities and angular resolutions well above the existing limit by exploiting the advantages of combining two state-of-the-art 8m-class mirrors on one common mount: The idea of the Large Binocular Telescope (LBT) came into reality [1]. Instruments should be able to combine the radiation from both telescopes in an either incoherent or coherent way. For this purpose, a suite of 10 first generation instruments at 12 existing focal stations has been selected and is currently under development or partly already in use at the telescope [2]. The whole LBT project is a joint enterprise between partners from the US (Arizona: 25%, Research Corporation: 12.5%, Ohio State: 12.5%), from Italy (INAF: 25%) and from Germany (LBTB: 25%). The MPIA leads a German-Italian consortium of scientific institutes, which are in charge of building the near-infrared (NIR) Fizeau-type beam combiner LINC-NIRVANA for the LBT [3]. Except for LBTI, the LBT Interferometer [4], which is designed for Fizeau interferometry/imaging and nulling interferometry/coronography in the mid-infrared spectral range, LN is the only instrument, which will use the full binocular capability of the telescope.
This paper is structured in the following way: Section 2 gives a technical overview of the telescope and the instrument, explains the principles of Fizeau interferometry and multi-conjugate adaptive optics, introduces LN's hardware architecture and compiles its main performance figures in a summarizing table. Section 3 outlines the currently ongoing AIV program the instrument has to successfully pass in the next few years before Acceptance Europe and commissioning on Mt. Graham. Section 4 focuses on managerial and system-engineering tools applied by the LN team to cope with the overall programmatic complexity. Section 5, finally, explains how step-wise commissioning allows switch-in of gradually increasing complexity over the years and gives a forecast of potential first science goals.

2. TECHNICAL OVERVIEW

2.1 LBT

The LBT comprises the world's first arrangement of two 8m-class Gregorian telescopes on one common mount, see Figure 1. This setup mimics the light gathering capability of a single 11.9m telescope (combined area of both primary mirrors) with the angular resolution of a 22.8m telescope (maximum aperture). The whole system allows for horizontal and vertical motion relative to a local reference, making the LBT a classical alt-azimuth configuration. An important feature emerging from this is the required de-rotation of all sky fields to avoid image smearing on any long scientific exposure. Basic properties of the LBT can be found in Table 1.

Table 1: General properties of the LBT.

Property	Feature or performance value/estimate	Notes
Observatory general (LBT)		
Site	Mt. Graham, Arizona, USA. W 109°53'20.63'' , N +32°42'04.71'' Altitude: 3221m, mean sidereal time: MST = UTC – 7hours	
Prime aperture	2 x 8.4m (binocular) on one common alt-azimuth mount	
Configuration	Gregorian, comprising prime focus with F/1.14 and secondary focus with F/15	LN uses the secondary focus (see Figure 1)
Modes of operation	1. Two independent 8m-class telescopes 2. Incoherent combination (light gathering capability of an 11.9m telescope) 3. Coherent combination (interferometry along the 14.4m baseline)	LN uses this 3rd mode
Focal stations	Prime foci – used by LBC-Blue and LBC-Red Secondary direct foci – used by MODS 1+2, PEPSI polarimeter 1+2 Secondary bent foci, front – used by LUCI 1+2 Secondary bent foci, middle – used by LBTI Secondary bent foci, rear A – used by LINC-NIRVANA Secondary bent foci, rear B – used by PEPSI spectrometer 1+2 fibers	For more details about instrumentation, see [2]
Operating temperature	-10°C to +25°C	This range is specified for LN

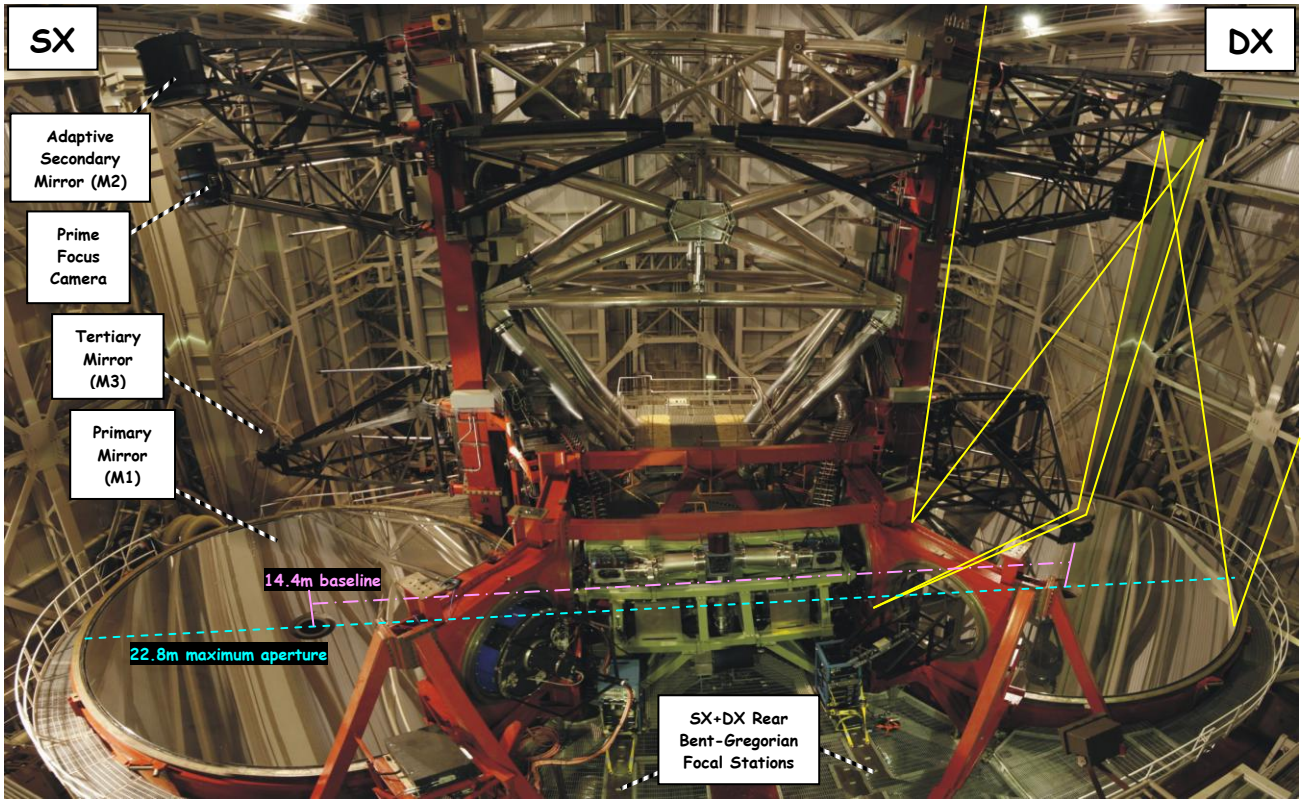

Figure 1: The Large Binocular Telescope. Two identical and symmetric Gregorian configurations are implemented on one common mount, which allows for alt-azimuth motion. SX and DX denote the left and right side, respectively. On the DX side, the principal light path is illustrated (in yellow) to identify the positions of the prime focus (where dedicated cameras can be turned-in) and the secondary bent focus. The latter can pass through the hole in the primary or be relayed via the tertiary mirror to three different positions on the instrument platform in the middle. LINC-NIRVANA will use both (SX + DX) rear foci once it is installed. (Photo: Courtesy of T. Ruppel, University of Stuttgart).

2.2 LINC-NIRVANA

LINC-NIRVANA (full version: "LBT INterferometric Camera and Near-InfraRed / Visible Adaptive iNterferometer for Astronomy"; short version: LN) is conceived as a near-infrared imager, which allows on the one hand the coherent superposition of light from both single-eye telescopes on a single science detector. The interferometric principle rests on the so-called "sparse aperture imaging" technique [5], which was invented by the French physicist Hippolyte Fizeau in 1867: Masking a telescope in such a way that only two small apertures (holes) allow the light to pass and produce interference fringes will drastically increase the angular resolution along the baseline of the two holes. The corresponding configuration is therefore often (and also in this paper) referred to as "Fizeau interferometer", although this term is often also used in conjunction with (1) the famous 1851 experiment supporting the development of special relativity and (2) apparatus used to characterize the quality of optical surfaces. Moreover, the overall geometry has to be preserved in order to mimic a Fizeau interferometer by combination of two independent telescopes-instrument sides (as in the case of LBT-LN): The instrument's two-fold exit pupil (right before combination) has to be a scaled version of the telescope's two-fold entrance pupil (feeding the instrument) [6]. This so-called "homotheticity condition" makes the instrument rather a "homothetic imaging system" (combination of separated telescopes) than a pure Fizeau interferometer (aperture masking of a single telescope). Only in this case, interference in the focal plane will preserve phase information across a large field of view (FOV). While the image in a single-eye, diffraction-limited exposure of a point source is given by the rotationally symmetric Airy pattern (the ideal point-spread-function, PSF), the dual-eye Fizeau pendant adds the 1D interferometric component emerging from the 14.4m baseline, thus sampling at a higher spatial frequency, and hence resulting in an increased angular resolution in this direction. This behavior and also its sensitivity under relative phase shifts is illustrated in Figure 2.

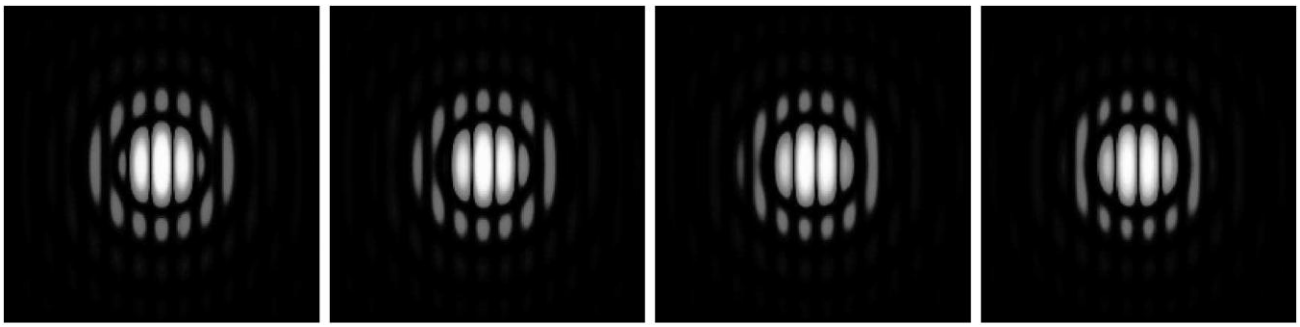

Figure 2: Simulated monochromatic PSFs for the interfering SX and DX beams. The usual 2D rotationally symmetric Airy pattern emerging from the diffraction in single-eye mode (one of the two 8.4m telescopes) is modulated with a higher spatial frequency by the additional Fizeau-type interference of both eyes (1D, along the 14.4m telescope baseline). Both patterns (1D + 2D) change their relative position synchronously with the relative optical path difference (OPD) between both sides. In the given example OPD changes from 0 to λ/2 in equidistant steps (from left to right), and hence the central maximum turns into a central minimum. Note: A simple analog of LN's interferometric principle is realized in Young's double-slit experiment with circular holes instead of infinite slits: The modulus of the Fourier transform of the pupil function results in exactly the same interference figure as shown above.

The instrument allows on the other hand the application of the multi-conjugate adaptive optics principle (MCAO, [7]): While classical adaptive optics corrects only on-axis the integral wavefront distortion through all turbulent layers of the earths's atmosphere, LN's MCAO systems allow us to individually correct wavefront distortions originating from dynamic air-masses in ~100m (ground-layer) and ~7.2km (high-layer), respectively. The key benefit of this (layer-oriented) technique is a drastically increased FOV for the interferometric fringe tracking while only natural guide stars (NGS) are required. A possible future upgrade of LN even allows for a third (mid-) layer correction.
LN's overall technical concept is depicted in Figure 3, whereas the detailed design can be seen in Figure 4.

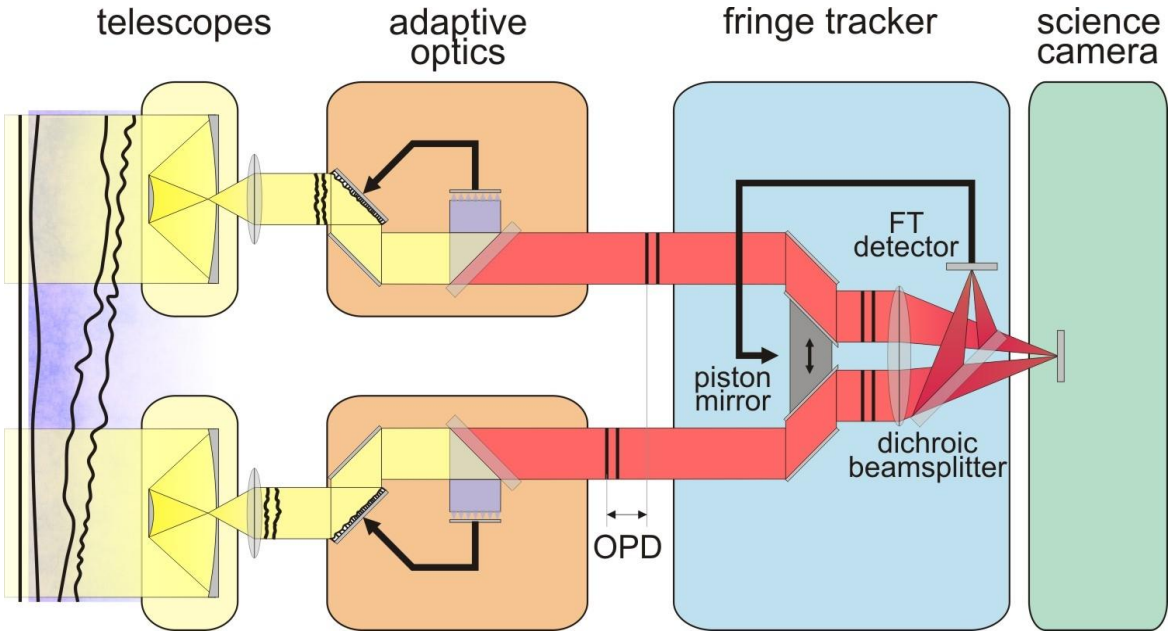

Figure 3: Technical concept of LINC-NIRVANA. From left to right: The unperturbed wavefront of the astronomical object suffers from atmospheric distortions (from high-frequency, local ripple up to low-frequency tip-tilt), before the two telescope halves are reached. Although coherence still exists between the parts hitting the SX and DX side of the LBT, the wavefronts need to be corrected in form and phase, before optimal interference becomes possible. The form, on the one hand, is corrected by the instrument's adaptive optics system comprising wavefront sensors and deformable mirrors working in real-time closed-loop operation. In the case of LN this is implemented via a 2-layer MCAO system (two sensors/mirrors per side, simplified to one layer here). The relative phase, on the other hand, is tuned by positioning a piston mirror to the balanced optical path difference (OPD) on both sides. In this case, the real-time closed-loop uses the interference pattern of the fringe tracking (FT) detector for feedback generation. The completely corrected and coherently superimposed wavefront finally falls onto the science detector.

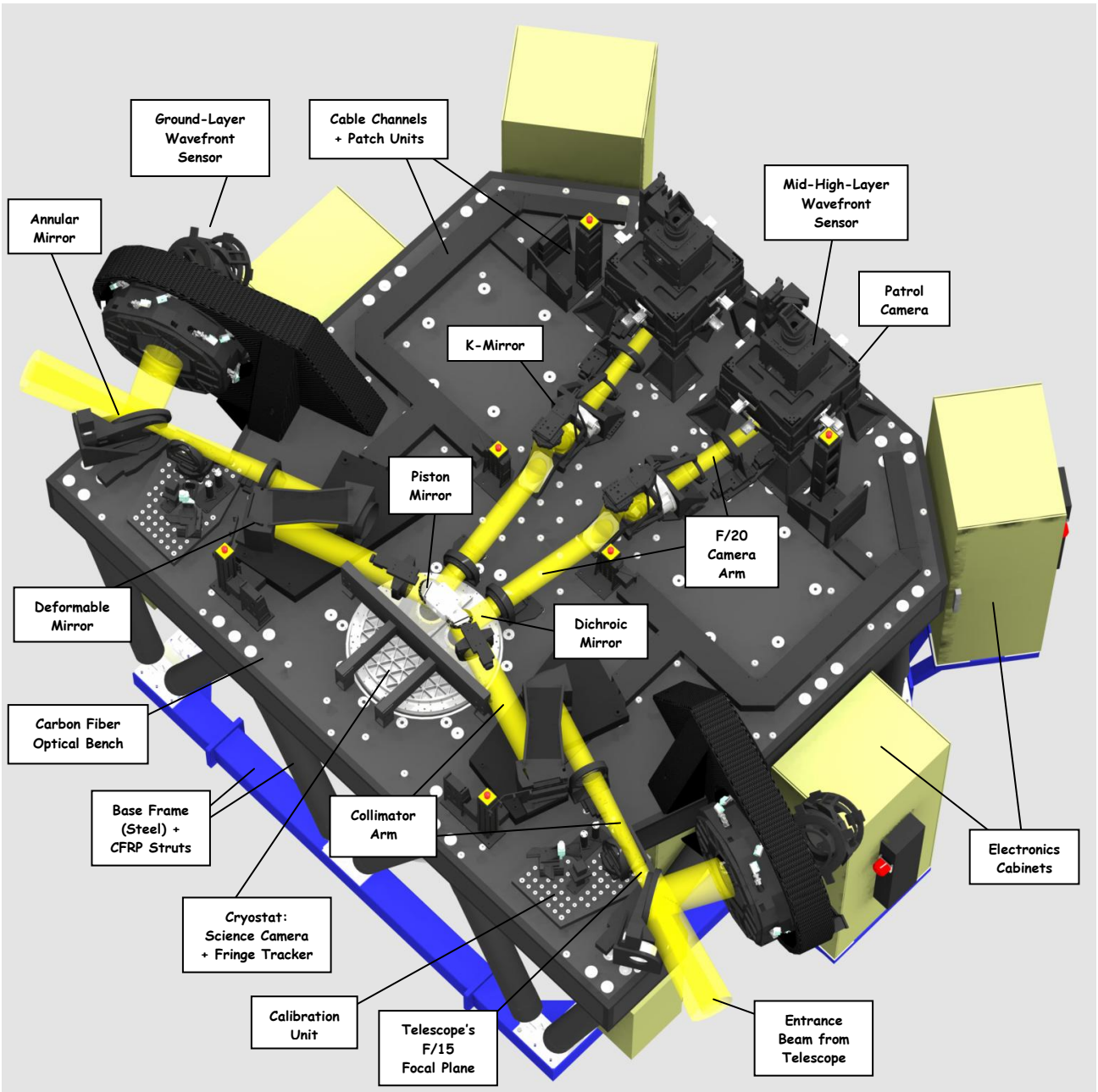

Figure 4: LINC-NIRVANA design overview. Note the complete left-right-symmetric configuration of this Fizeau-type interferometric imager. In addition to the populated optical bench, LN comprises also (1) a Stirling-type cryo-cooler linked via dedicated ~40m long isolated hoses for gaseous helium (at ~60K and 25bar) setting the required conditions for the science camera inside the cryostat, and (2) a suite of dedicated control and data acquisition computers.

While the instrument's lower part is realized as a steel base frame comprising the interface to the telescope's mounting platform at the rear bent-Gregorian focal station, the optical path with its sensitive components is installed on a carbon fiber reinforced plastic (CFRP) bench of low mass, high mechanical stiffness and high thermal stability. A system of 14 tunable CFRP struts links both parts of the instrument support structure and accounts for opto-mechanical stability and thermal decoupling. Light from the telescope's tertiary mirrors enters the instrument from the left and the right side simultaneously, see also Figure 1. Both beams run individually through two symmetric halves of the instrument before combination takes place in the cryogenic beam combiner.

The following description is therefore identical for the left (SX) and right (DX) part, respectively. After having entered the instrument, the beam hits an annular mirror slightly in front of the telescope focus. The portion in the 2 - 6arcmin annular field is reflected toward the ground-layer wavefront sensor (GWS), while the inner 2arcmin circular portion of the light continues its travel toward the beam combiner.

The GWS (sitting in its own de-rotator bearing) comprises a set of 12 pyramid star probes [8][9], which allow measuring the ground-layer atmospheric distortion of at most the same number of natural guide stars in this large field of view. Each pyramid star probe produces four enlarged, individual pupil images of the respective reference star with an intensity profile modulated by the atmospheric turbulence at the given layer. Calculating a gradient diagram from this 4-fold intensity profile allows decomposing the wavefront's turbulent information into a discrete spectrum of calibratable and orthogonal aberrations, the so-called Zernike modes. Feedback of this quantized information to the deformable mirror ultimately allows reconstructing the original, aberration-free wavefront.

Superimposing the signals of several selected natural guide stars (one per pyramid) by optical co-addition yields a higher signal-to-noise ratio and therefore allows the utilization of fainter guide stars for wavefront correction. This correction, in return, is done by the telescope's adaptive secondary, which translates the measured wavefront modulation into real-time (up to 1kHz) commanded counter-modulations of the mirror's deformable surface, which carries 672 individual voice-coil actuators [10].

Having also the main beam in the central 2arcmin simultaneously corrected in this way, it afterwards passes a collimator where two lens groups and a fold mirror group generate a parallel optical train with ~140mm of diameter. This fold mirror group not only accounts for a compact packing of the light path, but also one of the two flat mirrors is deformable (349 individual actuators) and used by the instrument's second, so-called mid-high-layer wavefront sensor (MHWS) for the second set of MCAO corrections, see below.

The parallel beam then hits the piston mirror, see also Figure 3, which is the essential component for balancing the phase information of both incoming wavefronts. By moving it along the optical axis, one beam is shortened, while the other is elongated, thus making the phase of the incoming wavefronts coherent, the vital prerequisite for interference on the science detector. The associated sensing and control instance in the corresponding closed-loop scheme, which allows for real-time corrections (up to ~100Hz) in this phase or optical-path-difference (OPD) direction, respectively, is the so-called fringe tracker of the interferometric camera, see below.

Directly after the piston mirror, a pair of dichroic mirrors separates the optical part of the beam (0.6 - 0.9µm) from the near-infrared (NIR) spectral component (1.0 – 2.4µm). The former enters the optical train of the MHWS, comprising an F/20 camera optics, a K-mirror for de-rotating the sky field, a patrol camera for position control and verification of the natural guide stars, and the wavefront sensor itself. The MHWS is able to select up to 8 of these targets out of the original 2arcmin circular field sky using the same pyramid-based technique as the GWS for generating corrective real-time signals, which –in this case– are post-processed by the deformable mirror in the aforementioned collimator branch of the instrument. The remaining NIR part of the beam finally enters the cryogenic camera and fringe tracking system, see Figure 5, where ultimately, the interferometric beam combination takes place.

The science camera (NIRCS, [11]) is embedded in a cryostat, which is cooled by gaseous helium at 60K and 25bar, as provided by a remote Stirling-type cryo-cooler. Having the two beams entering the cryostat at the right size and distance with respect to each other, i.e. in the required homothetic pupil condition as described above, the beam-combination itself is realized by an off-axis Cassegrain telescope (concave parabolic M1, convex hyperbolic and tip-tilt correctable M2). The convergent and interfering beams pass a dichroic wheel cryo-mechanism, which allows to separate the NIR once more into a reflected spectral component either in J (around 1.25µm), H (around 1.65µm) or K band (around 2.2µm) and the rest of the original band coming from the warm dichroics outside the cryostat, see above. This first component passes a filter wheel cryo-mechanism, which allows to select specific science-case relevant filters, and ultimately reaches the science detector (HAWAII-2, 2048 x 2048 pixels), which again sits on another de-rotating unit to account for the relative rotation of the astronomical target as seen from the alt-azimuth telescope mount.

The transmitted part on the other side of the dichroic enters the already mentioned fringe tracker, which uses the signature of the interfering beams to extract the relative phase information, which, in return, is required for real-time OPD corrections of the piston mirror (up to ~100Hz), see above. For this purpose a fringe tracker guide star is selected out of the corresponding 1arcmin x 1.5arcmin oval FOV and tracked very accurately by an XYZ-stage on the corresponding focal plane during the whole time of the scientific exposure. Since commercial stages of the required precision are not cryo-compatible, the lower part of the fringe tracker system is stabilized at ambient temperature, while the fringe detector (HAWAII-1, 1024 x 1024 pixels) itself is operating in the cold. A sophisticated baffle mechanism provides the thermal decoupling of both regions and preserves light tightness (to reduce radiative heat transfer) for the complete positioning range.

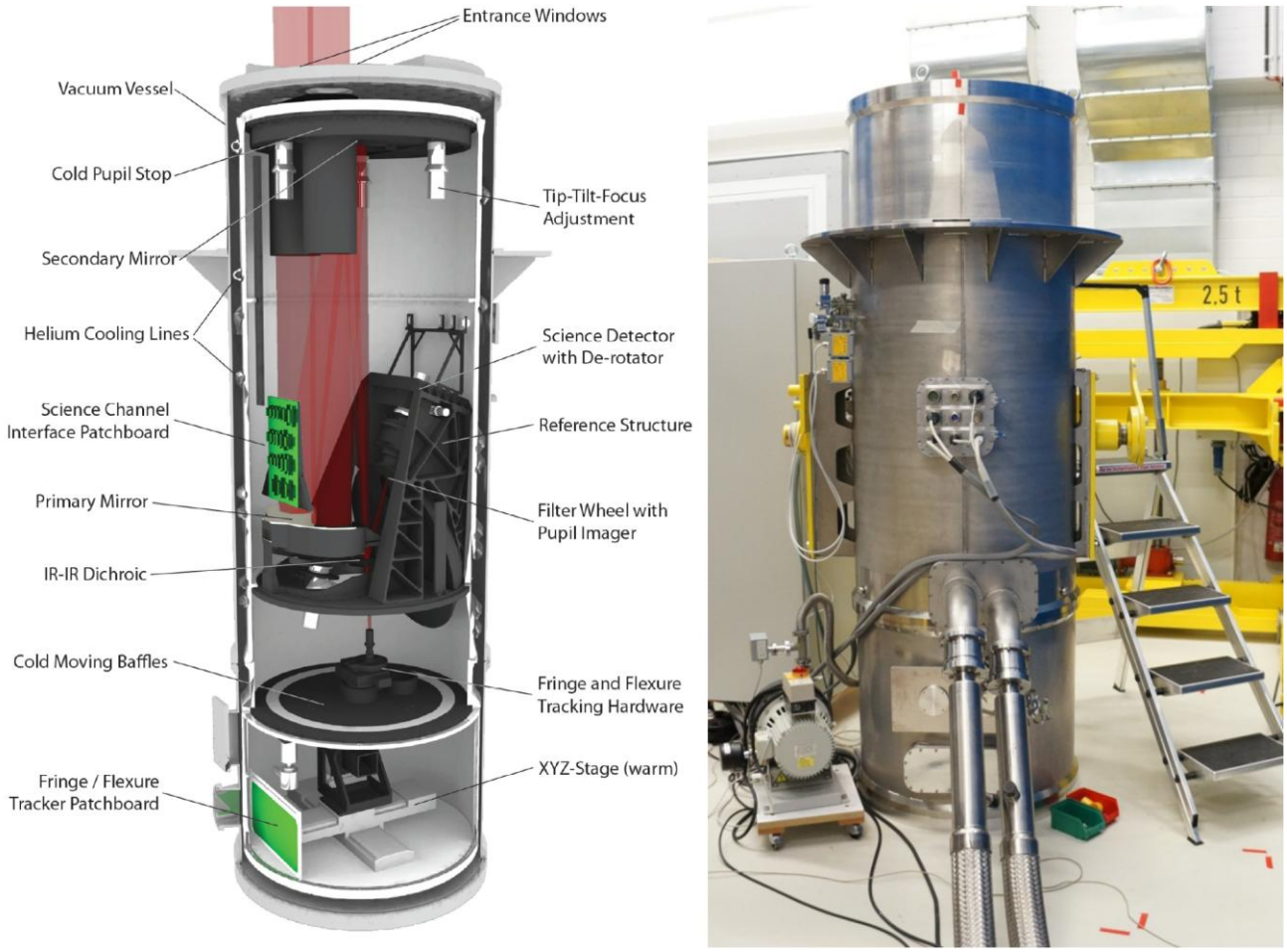

Figure 5: LINC-NIRVANA science and fringe tracker channel. The photo on the right shows also the helium cryo-hoses leading to the Stirling cryo-cooler, which in the final configuration will be ~40m away in a vibrationally isolated part of the telescope's dome.

Another cryogenic filter wheel in front of the fringe detector allows selection of the NIR band used for fringe tracking. In addition, throughput can be optimized by using filters with different coherence length.
A small periscope in the optical path of the fringe tracker is currently in the development phase. While in one channel of this periscope the main portion of the beams are superimposed for interferometry (on one quadrant of the detector), a smaller portion is bypassed through the second channel, where both individual beams are re-imaged as separated spots (on another quadrant of the detector). This allows detecting instrument flexure via the change in relative position of these spots. In this sense, the whole component is a fringe and flexure tracking system (FFTS, [12]). It should be mentioned that in a dedicated collaboration between the LN, LBTO (the managing institution of the telescope) and LBTI teams a so-called "OPD and Vibration Monitoring System" (OVMS) is currently installed at the LBT [13]. The purpose of this telescope facility is to measure all types of background vibrations in the range above ~10Hz. While the FFTS will detect atmospheric OPD modulations below this threshold, the OVMS will sense telescope-specific eigenmodes above it. A set of accelerometers mounted on the telescope mirrors and the two interferometers in conjunction with a real-time data acquisition and broadcasting system allows calculating the resulting parasitic OPD from the accelerometer signals. In LN's case the required correction is then commanded again via the piston mirror.

2.3 Performance capabilities

The following Table 2 summarizes the main properties of LINC-NIRVANA.

Table 2: LN's general features and performance capabilities.

Property	Feature or performance value/estimate	Notes
Instrument general (LINC-NIRVANA)		
Type	NIR Fizeau-type interferometric imager with MCAO capabilities	
Wavelength	1.0 – 2.45µm (J, H, K band) in science channel, 0.6 – 0.9µm for AO	
Science FOV	10.5arcsec x 10.5arcsec	
Angular resolution	10mas (J band) – 15mas (K band), perpendicular to azimuth pointing direction, extendable by observing the science field under different parallactic angles (so-called earth rotation synthesis)	Rotating fringe pattern assumed ~ parallel to detector columns
Maximum sky rotation per object	30° (+/- 15° of PSF rotation relative to detector columns), "per object" refers to one single science integration	Driver: Loss of fringe contrast
Min / Max zenith distance	Operation: 1.5° (sky de-rotation limit) – 60° (mechanical flexure limit) Survival: Full range 0° (zenith) – 90° (horizon)	
Minimum exposure time	0.55s, defining the lower limiting magnitude for bright objects to J = 8.9mag, H = 9.9mag and K' = 10.9mag to avoid detector saturation (without appropriate narrow-band filters)	Assuming: Double-correlated read on science detector
Maximum exposure time	10min, defining the upper limiting magnitude for faint objects to J = 26.9mag, H = 25.6mag and K' = 24.6mag, the latter at ≤ +5°C (assuming SNR = 5 with respect to background and Strehl = 40%; 10min apply only, if sky rotation limit is not exceeded)	Driver: Overall closed-loop stability + K-band background limit
MCAO channel 1 (GWS)		
GWS general characteristics	Static multi-pyramid wavefront sensor with associated field de-rotator (GWS bearing, integrated onto GWS)	One complete system per side (SX + DX)
Environment	Ambient	
FOV	Annular, between 2arcmin and 6arcmin diameter, the portion between 2arcmin and 2.88arcmin is partly vignetted	Provides LN's large sky coverage
Number of natural guide stars	Up to 12	Equivalent to the number of pyramids
Conjugated height	100m above telescope	
Associated deformable mirror	LBT's adaptive secondary mirror, 672 actuators	See also [10]
Sensor type	Scimeasure CCD50 (128 x 128 pixels, each 24µm x 24µm)	
Closed-loop performance	Up to 1kHz	
MCAO channel 2 (MHWS)		
MHWS general characteristics	Static multi-pyramid wavefront sensor with associated field de-rotator (K-mirror, separated from MHWS)	One complete system per side (SX + DX)
Environment	Ambient	
FOV	Circular, up to 2arcmin in diameter	Provides LN's large sky coverage
Number of natural guide stars	Up to 8	Equivalent to the number of pyramids
Conjugated height	7.2km	High-layer part (mid-layer designed for ~4km, but not yet implemented)
Associated deformable mirror	LN's internal DM (type Xinetics), 349 actuators	
Sensor type	Scimeasure CCD39 (80 x 80 pixels, each 24µm x 24µm)	
Closed-loop performance	Up to 1kHz	

Science channel (NIRCS)		
NIRCS general characteristics	Cryogenic, beam-combining camera with associated field de-rotator (detector unit, integrated onto science detector)	
Environment	Cryo-vacuum, 60K (stabilize-able to +/- 1K in the range 50 – 100K)	
FOV	Square, 10.5arcsec x 10.5arcsec	
Detector type	Rockwell/Teledyne HgCdTe HAWAII-2 PACE FPA (2048 x 2048 pixels, each 18µm x 18µm)	
Fringe and flexure tracker channel (FFTS)		
FFTS general characteristics	Combined cryogenic/ambient camera with cold detector and warm positioning unit for zero fringe tracking; a second detector quadrant is illuminated by a periscope to record beam drifting due to instrument flexure	The FFTS comprises NO field de-rotator to preserve the relative orientation of PSF to telescope baseline
Environment	Same as NIRCS (cryo-vacuum, 60K), only the detector positioning unit thermally decoupled to ambient temperature via a moving baffle	
FOV	Oval, 1arcmin x 1.5arcmin (with some vignetting)	
Number of natural guide stars	1	Limiting magnitude restricts LN's large sky coverage
Associated corrective element	LN's internal piston mirror with an overall OPD correction range of 150µm	
Detector type	Rockwell/Teledyne HgCdTe HAWAII-1 FPA (1024 x 1024 pixels, each 18.5µm x 18.5µm)	
Closed-loop performance	Fringe tracking: up to 100Hz Flexure tracking: ~ 1Hz	Driven by piston mirror's 1st eigenmode
OVMS detection limit	An OPD of λ/5 in J band = 250nm (goal: λ/10 = 125nm) in the range 10Hz – 100Hz	

3. AIV PROGRAM

LINC-NIRVANA passed its Final Design Review (FDR) in 2005. The current planning results in a Preliminary Acceptance Europe (PAE), i.e. the acceptance review which needs to be passed before shipment to the LBT, by the end of 2014. The following chapters describe the assembly, integration and verification (AIV) roadmap and the related milestones to reach this goal.

3.1 Integration hierarchy

To cope with its complexity, LINC-NIRVANA is subdivided into different integration levels. The consortium is organized in such a way that individual partners develop units or sub-systems in their respective field of expertise. They run through a thorough test program before a dedicated acceptance process checks the readiness for the next higher level. In this way a set of more than 20 sub-systems comprising an even higher number of units faces system level integration at the PI institute in Heidelberg. Following this scheme, the complete instrument is structured into the 4 already mentioned main systems (NIRCS, MHWS, GWS and FFTS), a common hardware part which comprises the optical bench and the electronics cabinets for instance and some auxiliary hardware like AIV tools and simulators for the turbulent atmosphere (MAPS) or the piston between both sides of the telescope. Furthermore, each system has its own software package, which is linked to common software modules responsible for instrument control or the interaction with the telescope. This whole scheme is summarized in tabular form in Figure 6.

Telescope						
LINC-NIRVANA						
NIRCS	**MHWS**	**GWS**	**FFTS**	**common HW**	**auxiliary HW**	**common SW**
Cryostat and Cryocooler	Collimators	Annular Mirrors	Piston Mirror	Bench	LN MAPS	LOSS
NIR Opto-Mechanics	Warm Dichroics	GWS Sensors	FFTS Detector	Cabinets	Alignment Tools	LICS
Science Detector	FP20 Optics	GWS Testbed (Pathfinder)	FFTS Sensor	Calibration Units	Piston Simulator	LBCS
	K-Mirrors		OVMS	Computer Architecture		LTCS
	Patrol Cameras			Services		LCALS
	MHWS Sensors					
LIRCS	LAOS	LAOS	LFFTS			

Figure 6: Integration hierarchy for LN from sub-system and system up to instrument and telescope level. The lower and rightmost entries represent the corresponding software modules.

3.2 Verification approach

For each sub-system (for instance the K-Mirrors or the Warm Dichroics as shown in Figure 6), a set of preliminary performance requirements and interfaces was defined for the FDR in 2005. With this basic information, the development of those standalone components could be advanced and mostly completed in the past years. As mentioned before, a dedicated acceptance process (for more details, see below), through which each hardware and software sub-system has to run, marks the natural end at this level and provides the qualification for the next higher one, i.e. system level.
The whole system level AIV approach has been worked out in 2010/2011 and was reviewed by independent experts from LBTO and ESO in June 2011. The corresponding scheme is depicted in Figure 7.

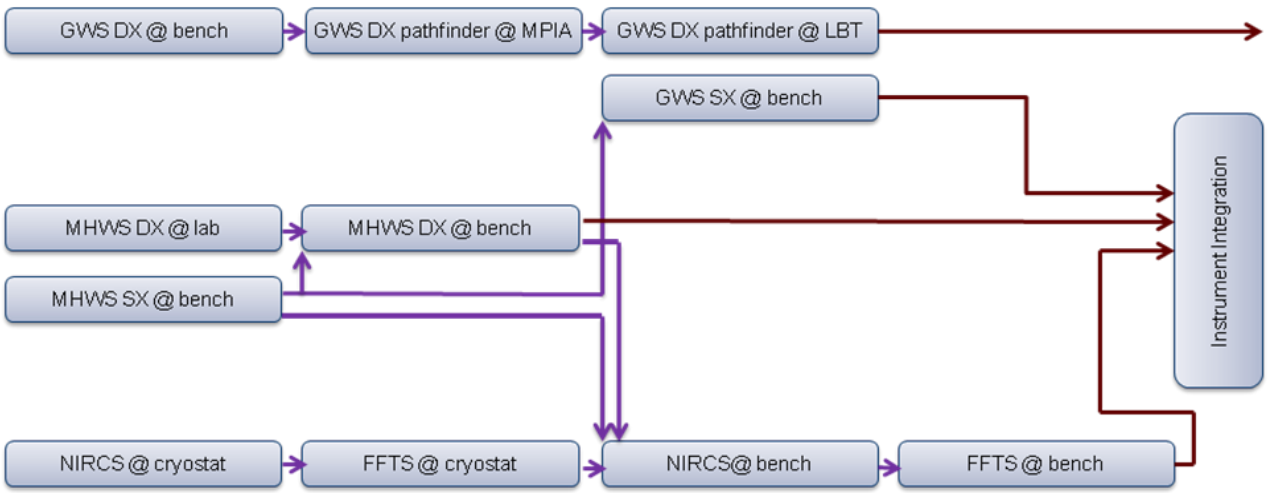

Figure 7: LN's system level AIV phases.

This scheme relates the four systems defined above to self-contained AIV phases, which are represented by individual boxes. This approach allows the splitting of complexity and available resources (integration halls, laboratories, AIV teams) into natural and manageable campaigns with the following AIV goals:

- The GWS DX branch characterizes the ground-layer system. Here the "@ bench"-phase allows for flexure characterization of the sensor by using the telescope's tilt simulator of LN's optical bench, see Figure 8. In the subsequent phases, the whole system is set up in a dedicated test-bed, the so-called "GWS DX Pathfinder" [14], see also Figure 8, which will be shipped in early 2013 to the LBT for a first interface and performance verification. GWS SX will benefit from this experience much later in the program.
- The MHWS DX branch starts with a dedicated campaign in MPIA's AO laboratory, see Figure 9, where the (mid-) high layer AO loop performance is optimized [15]. In parallel, the MHWS SX branch is built-up on LN's optical bench to verify the overall alignment concept, to check for interface compatibility and to establish an observatory-representative environment in MPIA's integration facility.
- The NIRCS and FFTS branch starts in the stand-alone cryostat, see Figure 5, with a focus on cryogenic, opto-mechanical end-to-end performance of individual components, on science detector optimization and on the choreography of the whole suite of sub-systems in the final environment. Subsequent phases "@ bench" ultimately complete the alignment concept and allow for the very first time to illuminate and combine both sides of the instrument from the collimator up to the science detector and fringe tracker. For this purpose, two on-axis and two off-axis coherent IR light sources of the calibration unit located at a re-imaged telescope's F/15 focal plane will be used.

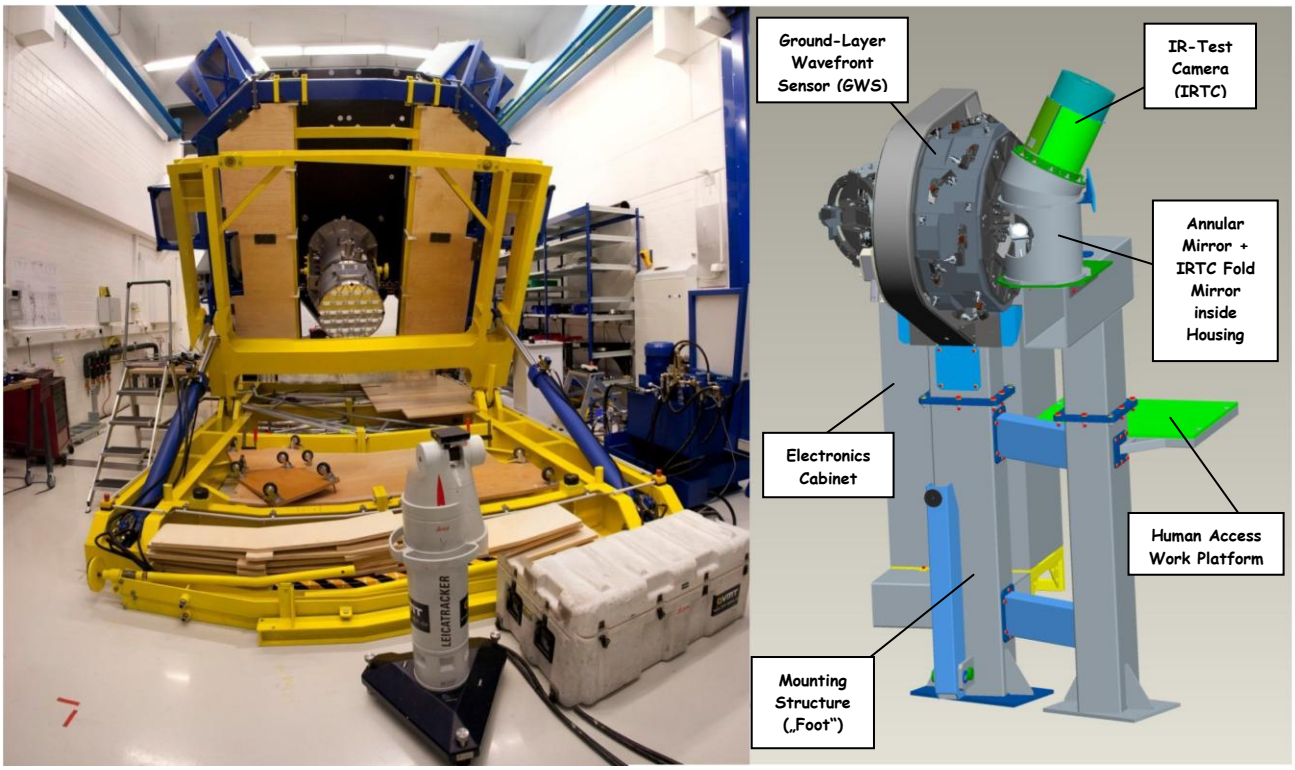

Figure 8: Left: The LN Optical Bench on its (tilted) telescope simulator in the MPIA integration hall. This setup is usually also used to characterize flexure of sub-systems like the GWS. This defines the "GWS DX @ bench"-AIV phase. Right: Once the sensor is checked for acceptable flexure it will be integrated into the GWS Pathfinder. This complete system will run through an extended test phase at MPIA before it is shipped to the LBT as the first item for instrument commissioning in the dedicated "GWS Pathfinder @ LBT"-campaign.

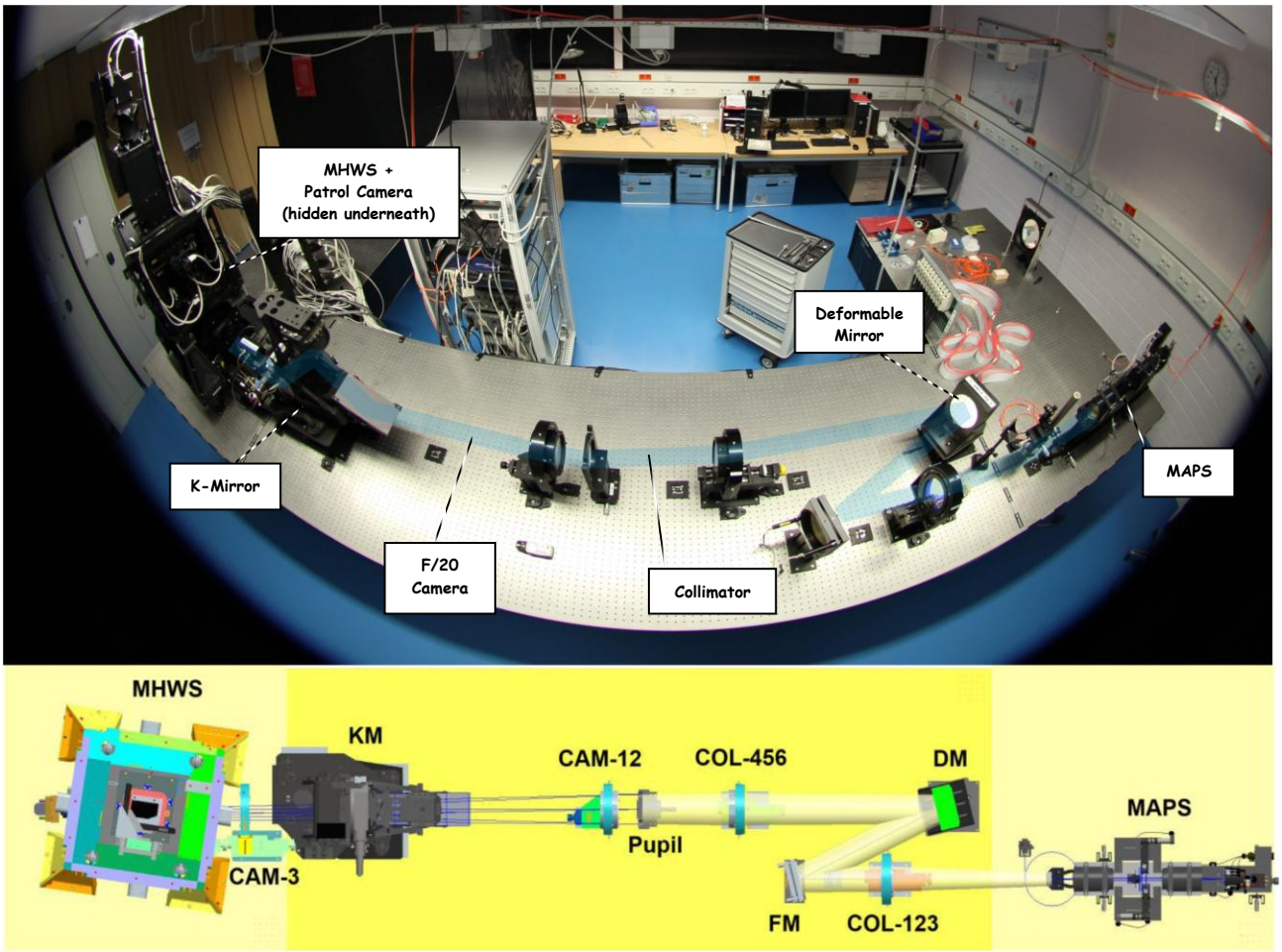

Figure 9: The LN lab setup serving the AIV phase "MHWS DX @ lab", which aims to optimize of the AO closed-loop operation. Crucial components of this subset of LN's complete right arm (compare Figure 4) are the optical telescope and atmospheric turbulence simulator MAPS, the MHWS together with its deformable mirror and the K-Mirror allowing for de-rotating the telescope's field of view (here simulated by rotating fibers within MAPS). The lower figure shows the optical train in more detail.

After completion of these system level phases, the instrument is practically integrated and aligned, and thus ready for a final set of instrument level tests. The main focus during this AIV-phase is to confirm the overall hardware-software compliance and to verify LN's performance stability under simulated, changing environmental conditions like telescope elevation, external vibrations (due to wind or other instrumentation) and ambient temperature.

4. COMPLEXITY MANAGEMENT

The sections above gave an introduction to the technical complexity of LINC-NIRVANA, its development and verification. In addition, in the first years of its operation, LN will have the status of a "strategic" rather than a "facility" instrument at the LBT. This means that also due to its operational complexity, the LN consortium will be fully responsible for running both instrument and telescope optics. As usual in instrumentation projects of this kind, technical challenges are accompanied by the fact that international teams need to be coordinated and resources need to be made available when required. In contrast to other scientific undertakings of comparable reputational impact and cost horizon, however, there is no major steering or controlling research institution like ESO or ESA in the background. This means in return, that there are no pre-defined or established managerial structures; hence the instrument team itself is responsible for both management and control management of its own development. To cope with this "non-existing-customer-situation", the LN consortium has tried to establish its own managerial and control tools, based on long-term experience with ESO- and ESA-standards. The next section describes control management tools as implemented for the overall long-term project planning as well as for an effective tracking of day-to-day tasks.

4.1 Project control tools

The AIV roadmap as depicted in section 3.2 has been converted into a thorough planning baseline, the LN AIV plan. All related phases, i.e. all the individual boxes in Figure 7, were subdivided by (1) an entry milestone comprising the readiness of all required components to start the integration, by (2) an intermediate milestone declaring completion of the integration process and readiness for verification and by (3) an exit milestone marking the successful completion of the verification process and formal acceptance of the related system for the next integration level. These milestones build up the system and instrument level skeleton of the LN master schedule. While there might be enormous sets of individual tasks in the respective integration and verification blocks of those phases, the milestones always allow for an effective and fast control mechanism of the overall progress and the identification of problems. In addition those milestones not only link the preceding and successive blocks, but also contain all dependencies toward sub-systems and cross-dependencies toward other system phases. The "only" additional information the master schedule has to provide is the listing of all involved work packages, the estimate of their duration and the assignment of adequate human resources. All consortium partners provide their input to the overall LN master schedule in that sense.

Control of the acceptance at the end of the verification phase is a vital element to guarantee that the maturity for the next integration level is really reached. To make a system work requires the functional performance of all its components and their correct interplay. In this sense, the most important acceptance process happens between sub-system and system level. Accordingly, an extra milestone has been introduced for each sub-system, which marks the successful completion of this acceptance process. The control mechanism in this case is a dedicated acceptance review, in which the LN partner responsible for the component has to provide a comprehensive documentation package to the receiving LN partner and/or other component-specific technical experts. This so-called Acceptance Data Package (ADP) follows a defined documentation standard and typically comprises a design report of the component (DES), a manual (MAN), an interface control document (ICD), a parts and spare parts list (PLI) and a verification report (VER), where details of all performed tests or analyses are collected and where – in a standardized verification matrix – the originally defined requirements are compared with the finally achieved test results. In this way, the enormous set of data can be controlled, archived and made available for any higher level assessment, like in an error budget or an interface inspection point.

Apart from tracking the achieved performance, this approach of a trans-level verification matrix allows us to establish a complete data base of verified requirements (component-specific) and interfaces (between two components) and hence it becomes possible to compare the originally defined, top-down science requirements with the finally achieved, bottom-up verification data to improve the overall performance forecast for the whole instrument, compare Table 2. Beyond this instrument internal verification control approach, LN's success crucially depends on the definition and control of all requirements and interfaces toward the telescope. Since the LBT is also still in its development phase, where fundamental issues like telescope flexure, background vibrations and binocular collimation need to be well understood, this requires an active exchange of information and a timely freeze of mutual dependencies between the LN consortium and LBTO. Accordingly, requirements and interfaces are controlled by two dedicated master documents governing the top-level interaction between instrument and telescope. For illustration purposes, Figure 10 gives an overview of topics, which are handled in the LN-LBT ICD for all applicable technical disciplines, i.e. mechanical, electrical, thermal, optical, software and service interfaces.

Another task of control management is the regular tracking of project related risks. This ranges from any technical risk, which might degrade the ultimate end-to-end performance of the instrument, up to programmatic risk related to availability of key personnel or project funding. For this purpose, the LN consortium has established a risk assessment process in 2010, which is updated in yearly mitigation control exercises. The outcome is compiled and maintained in a dedicated risk report. Due to the instrument's experimental character (no complete set of pre-defined requirements on all levels, late convergence of design details, some years of "strategic" co-existence of instrument and telescope) about half of the currently identified 50 risks are in the category "high risk". To retire or at least mitigate interface risks with the telescope, early test campaigns with subsets of the whole instrument are part of the planning. One example is the already mentioned GWS Pathfinder to gain first-hand experience with the interface to the telescope's adaptive secondary mirror, the telescope control system and the related software interaction. Instrument mockups were used in the past and might be also used in the future to verify mechanical envelope compliance with the telescope or to investigate the level of telescope flexure under different elevation angles and its impact on instrument internal stress or misalignment.

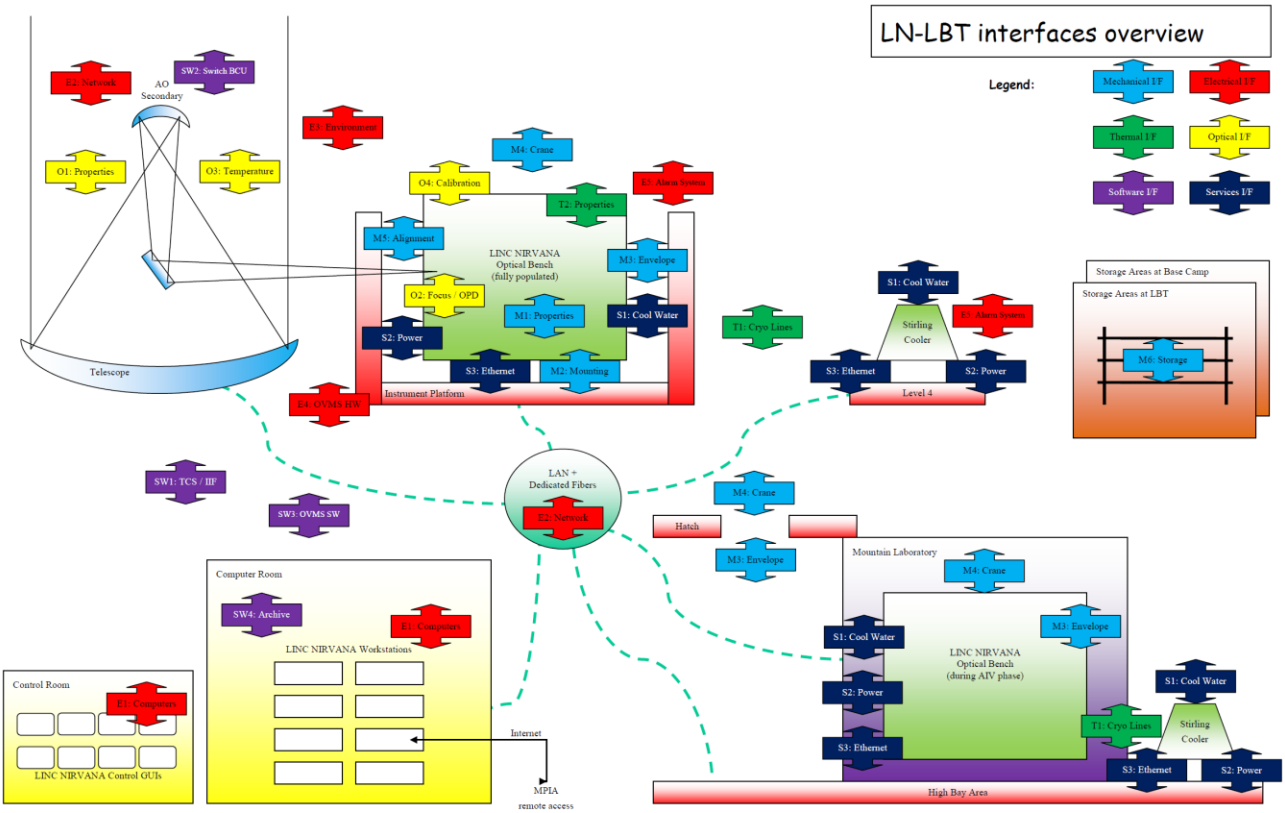

Figure 10: Interface management between the instrument and the telescope.

The detailed organization of tasks and the day-to-day communication within the LN consortium is supported by the web-based project management tool TRAC (Edgewall Software). This platform comprises the complete LN document and data archive, supports the overall planning by a ticket system, which allows to define and properly track every single work package in all its details and dependencies, and it allows to archive agreements or meeting minutes within an easily accessible and maintainable blog feature. Using in particular the ticket system in conjunction with the master schedule makes the daily work very efficient. Reporting the related progress within each ticket offers a valuable communication method within the whole LN consortium. In this way, a complex instrumental challenge with a complex distribution of work becomes manageable and predictable.

5. IMPLEMENTATION PHASES AND SCIENCE GOALS

Due to its technical and programmatic complexity as described above, also the commissioning of LINC-NIRVANA is split and will run through four implementation phases:

1. Demonstration of the GWS: This is the Pathfinder branch as described above. The goal is to verify working interfaces between the wavefront sensor system and its counterparts on the telescope side, comprising the adaptive secondary mirror as corrective element, but also the whole suite of other interfaces around the telescope's instrument platform and the related computer and networking infrastructure. This campaign is scheduled for early 2013 and will be completed by a first on-sky verification of the system's end-to-end performance, see [16].
2. LINC mode: The goal of this early full-instrument implementation stage is NIR interferometric imaging with just one on-axis NGS for fringe tracking and classical single-conjugate AO correction. Accordingly, the MHWS branch of the instrument will be used together with the telescope's adaptive secondary mirror, while the GWS and the instrument's internal DM are not in active operation. This campaign is currently scheduled for early 2015.

3. Demonstration of monocular MCAO: One of the two single-eye telescopes will be used in this non-interferometric mode to run GWS and MHWS branches simultaneously for full-MCAO performance (extended sky-coverage). This campaign follows a successful LINC mode operation.
4. NIRVANA mode: This final step completes the overall instrument commissioning with full interferometric and MCAO capabilities. On the time scale mentioned above this implementation stage will be reached roughly two years after shipment of the instrument to Mt. Graham, i.e. by the end of 2016.

While step 1 and 3 are primarily of engineering interest with a focus on instrument-to-telescope interfaces and performance optimization, step 2 and 4 have an initial set of science goals. The rest of this paper will focus on a few selected LINC mode cases to give the reader an understanding of how LINC-NIRVANA will be used in the first years of operation. It should be noted that this step 2 is further subdivided into two categories: "Early LINC mode", where target, AO and FFTS reference star are all the same object in H and K band and "Full LINC mode", where all three objects can be slightly separated by less than 5arcsec on sky with the aim of studying fainter objects, and this time also in J band.

In a comprehensive selection process out of more than 20 initial LINC science projects (Galactic, nearby galaxies and high redshift) four prime LINC case studies have been identified:

1. Stellar clusters including binaries ("Early LINC mode"): Objects in this category will make use of some of LN's unique capabilities and therefore will also help to optimize instrument performance. Attributes like crowded field, PSF extraction/variation, de-blending, separation, dynamic range and astrometry will be addressed in detail. Possible show cases could be northern sky objects similar to Westerlund 1, a paradigm for massive star formation due to the similar ages, compositions and distances of its constituents, see Figure 11.
2. Active galactic nuclei ("Early LINC mode"): Attributes in this category are extended + point source, dynamic range, broad band color + narrow band line imaging. A candidate in this field is the nucleus of the giant elliptical galaxy M87 in the Virgo cluster exhibiting a 5000 light-year long jet of high-energetic plasma.
3. High-redshift galaxies ("Full LINC mode"): This will allow addressing faint, extended sources, PSF extraction/variation and broad band color imaging.
4. Galactic center ("Full LINC mode"): In addition to the attributes identified above, this special science case will also investigate LN's capabilities for objects at the edge of LBT's observational window (close to horizon), like the center of our galaxy, the Milky Way. Beside the resolution required for high-precision astrometry, there is a special focus on high airmass (long path through the atmosphere) and limited freedom for selecting parallactic angles as needed for the mentioned earth rotation synthesis.

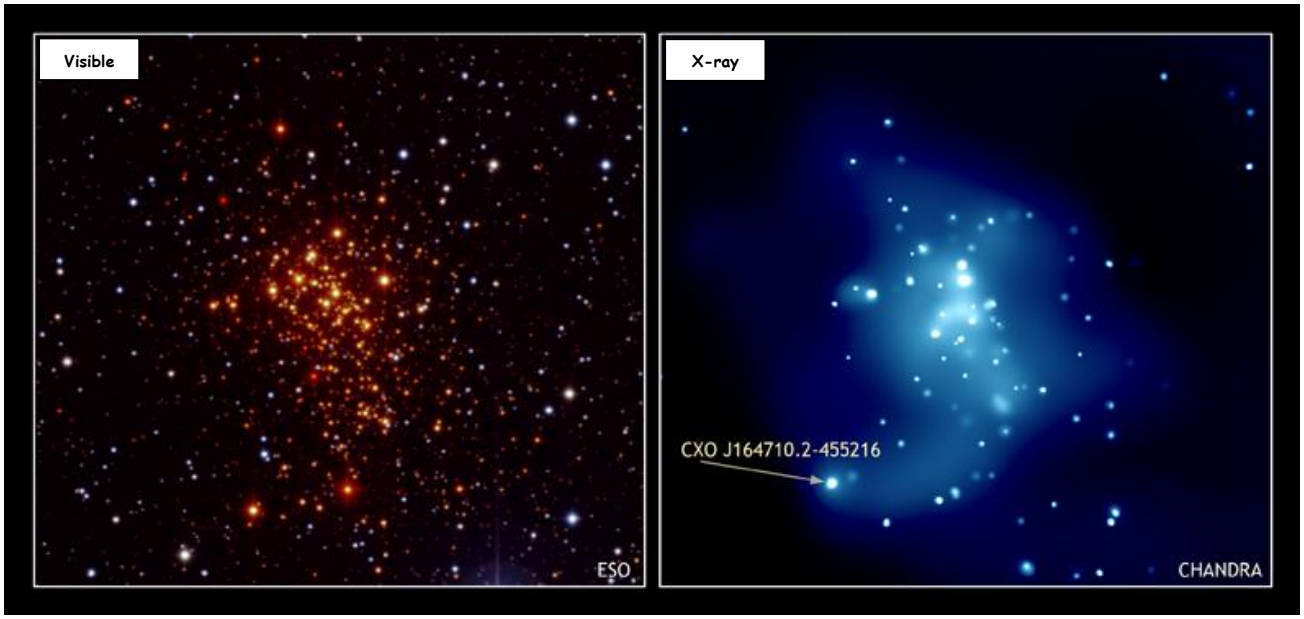

Figure 11: The compact, young and open stellar cluster Westerlund 1 (courtesy of NASA/CXC/UCLA/M.Muno et al.).

ACKNOWLEDGEMENTS

We would like to thank our partners at LBTO, in particular Richard Green, Joar Brynnel, John Hill and their teams, for the very close and effective collaboration since the beginning of the LINC-NIRVANA project. We are also grateful for working together with the INAF-Arcetri team on LN's interface toward the adaptive secondary mirror and with the LBTI team on the OVMS system as part of the telescope's infrastructure.

REFERENCES

[1] J. M. Hill, R. F. Green, D. S. Ashby, J. G. Brynnel, N. J. Cushing, J. Little, J. H. Slagle, and R. M. Wagner, "The Large Binocular Telescope", Proc. SPIE 7733, 77330C (2010).

[2] R. M. Wagner, "An overview of instrumentation for the Large Binocular Telescope", Proc. SPIE 7735, 773506 (2010).

[3] T. M. Herbst, R. Ragazzoni, A. Eckart, and G. Weigelt, "Imaging beyond the fringe: an update on the LINC-NIRVANA Fizeau interferometer for the LBT", Proc. SPIE 7734, 773407 (2010).

[4] P. M. Hinz, T. Bippert-Plymate, A. Breuninger, T. Connors, B. Duffy, S. Esposito, W. Hoffmann, J. Kim, J. Kraus, T. McMahon, M. Montoya, R. Nash, O. Durney, E. Solheid, A. Tozzi, and V. Vaitheeswaran, "Status of the LBT interferometer", Proc. SPIE 7013, 701328 (2008).

[5] T. A. Pauls, "Origins of sparse aperture imaging", Aerospace Conference, 2001, IEEE Proceedings, 3/1421.

[6] W. A. Traub, "Combining beams from separated telescopes", Appl. Opt. 25 (1986) 528.

[7] R. Ragazzoni, E. Diolaiti, J. Farinato, E. Fedrigo, E. Marchetti, M. Tordi and D. Kirkman, "Multiple field of view layer-oriented adaptive optics - Nearly whole sky coverage on 8 m class telescopes and beyond", A&A 396 2 (2002) 731.

[8] R. Ragazzoni, "Pupil plane wavefront sensing with an oscillating prism", J. Modern Opt., 43(2) (1996), 289.

[9] R. Ragazzoni, J. Farinato, "Sensitivity of a pyramidic Wave Front sensor in closed loop Adaptive Optics", A&A 350 (1999), L23.

[10] S. Esposito, A. Riccardi, E. Pinna, A. Puglisi, F. Quirós-Pacheco, C. Arcidiacono, M. Xompero, R. Briguglio, G. Agapito, L. Busoni, L. Fini, J. Argomedo, A. Gherardi, G. Brusa, D. Miller, J. C. Guerra, P. Stefanini, and P. Salinari, "Large Binocular Telescope Adaptive Optics System: new achievements and perspectives in adaptive optics", Proc. SPIE 8149, 814902 (2011).

[11] P. Bizenberger, H. Baumeister, T. Herbst, X. Zhang, "LINC-NIRVANA: Cryogenic optics for diffraction limited beam Combination", to appear in the proceedings of SPIE, Xiamen, 2012.

[12] T. Bertram, A. Eckart, B. Lindhorst, S. Rost, C. Straubmeier, E. Tremou, Y. Wang, I. Wank, G. Witzel, U. Beckmann, M. Brix, S. Egner, and T. Herbst, "The LINC-NIRVANA fringe and flexure tracking system", Proc. SPIE 7013, 701327 (2008).

[13] M. Kürster, T. Bertram, J. L. Borelli, M. Brix, W. Gässler, T. M. Herbst, V. Naranjo, J.-U. Pott, J. Trowitzsch, T. E. Connors, P. M. Hinz, T. J. McMahon, D. S. Ashby, J. G. Brynnel, N. J. Cushing, T. Edgin, J. D. Esguerra, R. F. Green, J. Kraus, J. Little, U. Beckmann and G. P. Weigelt, "OVMS: the optical path difference and vibration monitoring system for the LBT and its interferometers", Proc. SPIE 7734, 77342Y (2010).

[14] Conrad, A., Bertram, T., Kürster, M., Herbst, T., Ragazzoni, R., Farinato, J., Brangier, M., Viotto, V., Bergomi, M., Brunelli, A., Arcidiacono, C., Pott, J.-U., Bizenberger, P., Briegel, F., Hofferbert, R., Meschke, D., Mohr, L., Rohloff, R., Baumeister, H., De Bonis, F., Zhang, X., Trowitzsch, J., Berwein, J., Kittmann, F., "Status and plans for the LINC-NIRVANA Pathfinder," to appear in the proceedings of Second International Conference on Adaptive Optics for Extremely Large Telescopes, (2011).

[15] Zhang X, Gässler W, Conrad AR, Bertram T, Arcidiacono C, Herbst TM, Kürster M, Bizenberger P, Meschke D, Rix HW, Rao C, Mohr L, Briegel F, Kittmann F, Berwein J, Trowitzsch J, Schreiber L, Ragazzoni R, Diolaiti E, "First laboratory results with the LINC-NIRVANA high layer wavefront sensor", Opt. Express. 2011 Aug 15; 19(17):16087.

[16] A. R. Conrad, C. Arcidiacono, H. Baumeister, M. Bergomi, T. Bertram, J. Berwein, C. Biddick, P. Bizenberger, M. Brangier, F. Briegel, A. Brunelli, J. Brynnel, L. Busoni, N. Cushing, F. De Bonis, M. De La Pena, S. Esposito, J. Farinato, L. Fini, R. F. Green, T. Herbst, R. Hofferbert, F. Kittmann, M. Kürster, W. Laun, D. Meschke, L. Mohr, A. Pavlov, J.-U. Pott, A. Puglisi, R. Ragazzoni, A. Rakich, R.-R. Rohloff, J. Trowitzsch, V.

Viotto, X. Zhang, “LINC-NIRVANA Pathfinder: Testing the next generation of wave front sensors at LBT”, to appear in the proceedings of SPIE 8447-121, Amsterdam, 2012.